

Correlation between melting behaviour and polymorphism of syndiotactic polystyrene and its blend with poly(2,6-dimethyl-1,4-phenylene oxide)

Bo Ki Hong^a, Won Ho Jo^{a,*}, Sang Cheol Lee^b and Jungahn Kim^c

^aDepartment of Fiber and Polymer Science, Seoul National University, Seoul 151-742, Korea

^bDepartment of Polymer Science and Engineering, Kumoh National University of Technology, Kumi 730-701, Korea

^cDivision of Polymer, Korea Institute of Science and Technology, Seoul 130-650, Korea
 (Received 21 April 1997; revised 26 May 1997)

The melting behaviour of syndiotactic polystyrene (sPS) and its blend with poly(2,6-dimethyl-1,4-phenylene oxide) (PPO) was examined by differential scanning calorimetry (d.s.c.), and the polymorphism of sPS was also investigated by X-ray diffraction. Both pure sPS and sPS/PPO blends showed three melting endotherms under our crystallization conditions. When the d.s.c. results are compared with the X-ray patterns, it is suggested that the lowest and middle melting endotherms are due to the melting of β - and α -forms of sPS, respectively, whereas the highest melting endotherm comes from the melting of recrystallized sPS crystals formed during the d.s.c. scan. It is also observed that the recrystallization of sPS in sPS/PPO blends is disturbed by the presence of PPO. © 1998 Elsevier Science Ltd. All rights reserved.

(Keywords: melting behaviour; polymorphism; syndiotactic polystyrene/poly(2,6-dimethyl-1,4-phenylene oxide) blends)

INTRODUCTION

The multiple melting behaviour of semicrystalline polymers crystallized from the melt has been investigated extensively^{1–9}. Semicrystalline polymers such as poly(ethylene terephthalate)^{2,7} and polyamides^{8,9} are known to exhibit two or more melting endotherms. It was reported that the origin of multiple melting endotherms could be classified into three mechanisms, i.e. simultaneous melting, recrystallization and remelting^{1,2}; melting of different crystal structures^{3,4}; melting of different lamellar thickness^{5,6}.

Since syndiotactic polystyrene (sPS) with a very high degree of stereospecificity (> 96%) has been synthesized successfully by stereospecific polymerization¹⁰, there has been considerable interest in the characteristics of this new material^{11–22}. Improved mechanical properties are expected for sPS, especially at high temperature, due to its crystalline structure. Furthermore, a larger crystallization rate of sPS relative to that of isotactic polystyrene and its high tensile modulus lead to a potential engineering plastic. It has been reported that the polymorphic behaviour of sPS is very complex. Hence many studies on sPS have focused on the analysis of the crystal structure. Four major crystalline forms, α , β , γ , and δ , have been proposed. The α - and β -forms formed by molecular chains with a planar zigzag conformation (T_4) are primary crystalline polymorphs and can be produced by thermal treatment. The α - and β -forms are of particular interest, since the extended chain conformation imparts an inherently stiff chain backbone to the sPS leading to improved mechanical properties. The α -form

has been shown to exist in a hexagonal^{14,15} or perhaps rhombohedral¹⁶ structure, whereas the β -form forms an orthorhombic structure¹⁷. The γ - and δ -forms formed by molecular chains with a helical conformation (T_2G_2) can only be formed from solvent swelling of glassy sPS, and both forms have been known to have the same monoclinic crystal structure^{18,19}. The γ -form is a completely dried crystalline structure, whereas the δ -form is always formed in the presence of a solvent and seems to include some solvent molecules.

A few studies on sPS-based blends such as sPS/poly(vinyl methyl ether) (PVME) and sPS/poly(2,6-dimethyl-1,4-phenylene oxide) (PPO) have been reported in the literature^{23–27}. Studies on sPS/PVME and sPS/PPO blends have focused on the crystallization behaviour and miscibility of the blends. For instance, Guerra *et al.*²⁷ have reported that the polymorphic behaviour of melt-crystallized sPS is altered by blending with PPO which strongly favours the β -form. However, systematic studies of the melting behaviour of sPS and its blend with PPO, which is essential for understanding the properties of semicrystalline polymers, are still lacking. In this study, we have investigated the nature of the multiple melting behaviour of sPS and its blend with PPO. The multiple melting behaviour is correlated with the polymorphism of the sPS crystal.

EXPERIMENTAL

Materials and blend preparation

The sPS ($M_w = 3.6 \times 10^5 \text{ g mol}^{-1}$, $T_g = 100.2^\circ\text{C}$,

* To whom correspondence should be addressed

$T_m = 271.0^\circ\text{C}$) was obtained from Idemitsu Kosan Co. Ltd., Japan. The PPO ($M_w = 4.5 \times 10^4 \text{ g mol}^{-1}$, $T_g = 219.1^\circ\text{C}$) was supplied by the Nippon Polyester Co. Ltd., Japan. The sPS/PPO blends were melt-mixed and injection-moulded in a Mini-Max moulder (CS-183 MMV, Custom Scientific Instruments, Inc.) at 300°C for 7 min.

Calorimetric measurements

A Perkin-Elmer DSC 7 differential scanning calorimeter was used for the thermal analysis. All scans were run under a nitrogen gas purge to minimize thermo-oxidative degradation. To determine the miscibility of sPS/PPO blends from the glass transition temperature, the samples were first heated from room temperature to 300°C , held at this temperature for 5 min to ensure complete melting of sPS crystals, and then quenched to room temperature. The samples were immediately reheated up to 300°C at a heating rate of $20^\circ\text{C min}^{-1}$. To examine the melting behaviour of the sPS/PPO blends, all specimens were isothermally crystallized in the DSC at various crystallization temperatures (T_c) for 60 min. After the isothermal crystallization was completed, the samples were heated from T_c to 300°C at various heating rates (5, 10, 20, or $40^\circ\text{C min}^{-1}$).

X-ray analysis

For the wide-angle X-ray diffraction (WAXD) experiment, samples were heated at 300°C for 5 min in a heating block, and rapidly transferred into another heating block previously thermostated at a given T_c , followed by isothermal crystallization for 60 min. After the isothermal crystallization was completed, the samples were quenched in a liquid nitrogen bath. The samples were analysed with a diffractometer (MAC MXP18A-HF) at a scanning rate of 5°min^{-1} . WAXD patterns were obtained with nickel-filtered $\text{Cu K}\alpha$ radiation. According to the method of Guerra *et al.*¹¹, the content of the two crystalline forms (α and β) present in the melt-crystallized samples was quantitatively determined. The percentage content of the α -form (P_α) can be evaluated by the following relation

$$P_\alpha = \frac{1.8A(11.6^\circ)/A(12.2^\circ)}{1 + 1.8A(11.6^\circ)/A(12.2^\circ)} \times 100 \quad (1)$$

where $A(2\theta)$ is the area of the peak located at 2θ (scattering angle), and 1.8 is the ratio between the intensities of the peaks at 11.6° and 12.2° for samples of equal thickness and crystallinity.

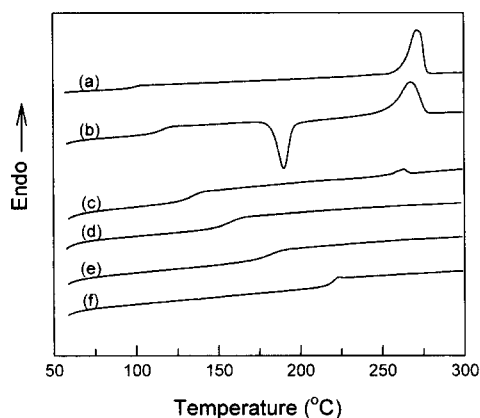


Figure 1 D.s.c. thermograms of sPS/PPO blends: (a) 100/0; (b) 80/20; (c) 60/40; (d) 40/60; (e) 20/80; (f) 0/100

RESULTS AND DISCUSSION

Miscibility

To investigate the miscibility of sPS/PPO blends, the glass transition temperatures were measured by the d.s.c. scan. Figure 1 shows the d.s.c. thermograms of sPS/PPO blends at a heating rate of $20^\circ\text{C min}^{-1}$. It is observed that sPS/PPO blends exhibit single composition-dependent T_g s, indicating the miscibility of the blends over entire compositions. The result is consistent with other previous reports^{25,27}. The sPS/PPO (80/20) blend shows an exothermic crystallization peak at 190.1°C , followed by a melting endotherm at 271.0°C . As the amount of PPO exceeds 60 wt%, there are no melting endotherms in the d.s.c. thermograms, indicating that the crystallization of sPS is hindered by addition of PPO. Figure 2 shows the composition dependence of the glass transition temperature for sPS/PPO blends. These data can be analysed by the Gordon–Taylor equation²⁸:

$$T_g = \frac{w_1 T_{g1} + k w_2 T_{g2}}{w_1 + k w_2} \quad (2)$$

where T_g is the glass transition temperature of the blend, w_i is the weight fraction of component i , T_{gi} is its glass transition temperature, and k is an adjusting parameter related to the degree of curvature of the T_g -composition diagram. The full curve represents the best fit to the Gordon–Taylor equation. The parameter k could be taken as a semiquantitative measure of the strength of interaction between the functional groups of the components of the blends^{29,30}. From the best fit of equation (2), the value of k is determined to be 0.578 which is similar to that of poly(bisphenol-A hydroxy ether)/poly(ethylene oxide) blends³¹.

Melting behaviour

Figure 3 shows the d.s.c. melting curves of pure sPS and the sPS/PPO (80/20) blend isothermally crystallized at various crystallization temperatures. All samples exhibit three melting peaks, i.e. the lowest melting endotherm (denoted by 'endotherm I'), the middle melting endotherm (denoted by 'endotherm II'), and the highest melting endotherm (denoted by 'endotherm III'). It is observed that the position of the melting endotherms varies significantly with crystallization temperature. In both pure sPS and the sPS/PPO (80/20) blend, the peak temperatures of both endotherms I and II shift to higher temperature as the

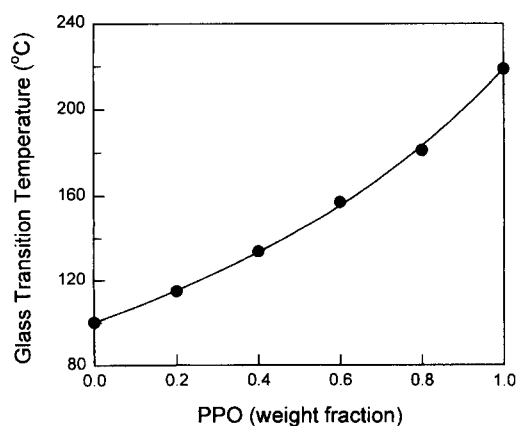


Figure 2 Composition dependence of the glass transition temperatures of sPS/PPO blends. The curve represents the best fit to the Gordon–Taylor equation

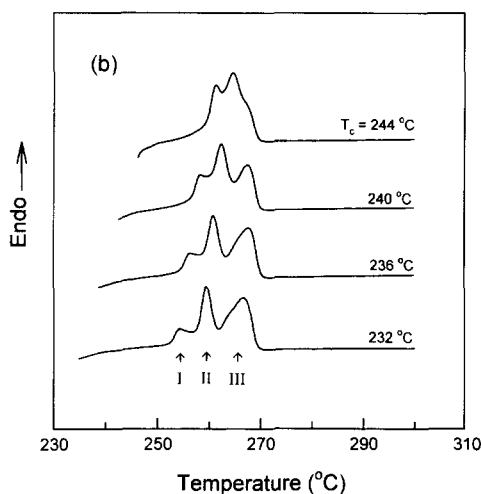
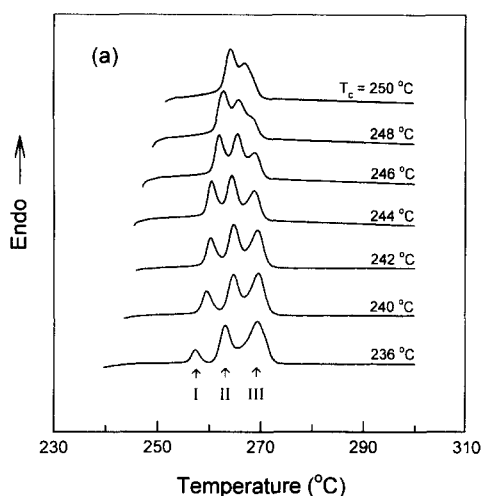


Figure 3 D.s.c. melting curves of samples crystallized at various crystallization temperatures when the samples are heated at $10^{\circ}\text{C min}^{-1}$: (a) sPS; (b) sPS/PPO (80/20) blend

T_c increases, while the peak temperature of endotherm III remains almost constant independent of T_c . It is also shown that the peak area of endotherm I relative to that of endotherm II increases with increasing T_c , while the peak area of endotherm III decreases with increasing T_c . At higher T_c s, the crystallization proceeds at a slower rate, resulting in more perfect crystals. Thus the fraction of crystals which would undergo reorganization on heating decreases with increasing T_c . In this aspect, one may conclude that the endotherm III arises from the melting of recrystallized sPS crystals. At the crystallization temperature of 244°C , the sPS/PPO (80/20) blend shows two melting endotherms with a small shoulder, while pure sPS clearly exhibits three endotherms with the melting peak of recrystallized sPS crystals. This result implies that the presence of PPO disturbs the recrystallization of sPS. It is well known that sPS exhibits polymorphic behaviour depending on the crystallization conditions^{11–21}. Specifically, the α - and β -forms could be formed by melt crystallization. Therefore, it is assumed that endotherms I and II may be due to the melting of two different crystal forms (α or β). This will be verified in the following section by comparing d.s.c. results with WAXD patterns.

To gain further insight into the above observation, the effect of the heating rate on the melting behaviour was investigated. *Figure 4* shows the melting curves of sPS and the sPS/PPO (80/20) blend crystallized at 240°C when the

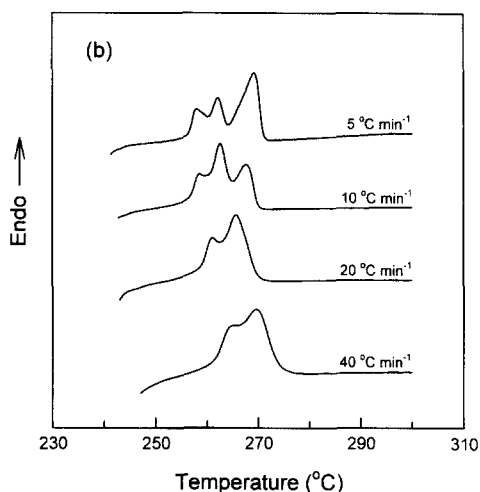
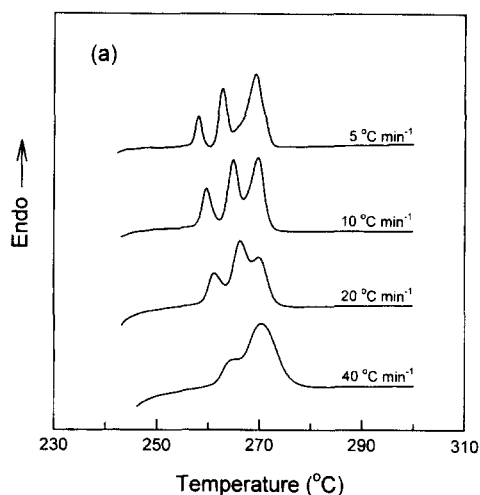


Figure 4 D.s.c. melting curves of samples crystallized at 240°C when the samples are heated at various heating rates: (a) sPS; (b) sPS/PPO (80/20) blend

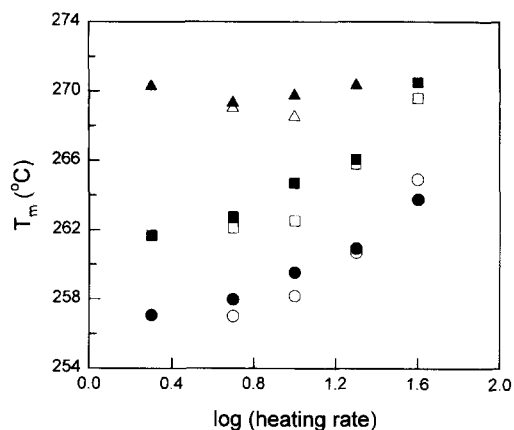


Figure 5 Melting temperature versus logarithm of heating rate for sPS and sPS/PPO (80/20) blend crystallized at 240°C . The circles, squares, and triangles represent the melting temperatures of endotherms I, II, and III, respectively. The filled and open symbols denote the pure sPS and the sPS/PPO (80/20) blend, respectively

samples are heated at various heating rates. As the heating rate is increased, the melting temperatures of both endotherms I and II increase, while that of endotherm III remains almost constant (see *Figure 5*). In addition, the peak area of the endotherm III gradually decreases with increasing heating rate. Generally, the crystals might have

less time to reorganize as the heating rate is increased, and consequently the peak area due to both recrystallization and remelting becomes smaller. Therefore, it is obvious that the endotherm III comes from the remelting of recrystallized sPS formed during the d.s.c. scan. When the samples are heated at a heating rate of $20^{\circ}\text{C min}^{-1}$, the melting curve of pure sPS exhibits three melting endotherms, whereas the remelting endotherm of the sPS/PPO (80/20) blend completely disappears, resulting in two endotherms. This result also supports the fact that the PPO in the blends disturbs the recrystallization of the sPS.

X-ray analysis

Figure 6 shows the WAXD curves of sPS and the sPS/PPO (80/20) blend crystallized at various T_c s. The two peaks at $2\theta = 11.6^{\circ}$ and 12.2° are assigned to the characteristic peaks of the α - and β -forms, respectively¹¹. In both pure sPS and the sPS/PPO (80/20) blend, the sPS crystals are always a mixture of α - and β -forms under our crystallization conditions. The characteristic peak intensity of the β -form relative to that of the α -form gradually increases with increasing crystallization temperature, indicating an increase in the amount of the β -form. When the melting behaviour of Figure 3 is compared with the behaviour of the WAXD pattern in Figure 6, it is concluded that the endotherms I and II correspond to β - and α -forms, respectively.

From the WAXD patterns, the percentage content of the

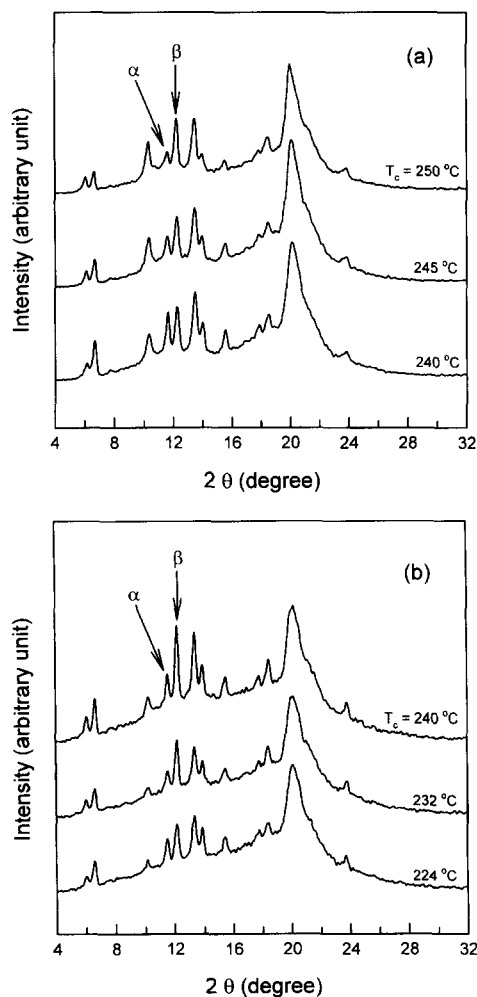


Figure 6 WAXD patterns of samples crystallized at various crystallization temperatures: (a) sPS; (b) sPS/PPO (80/20) blend

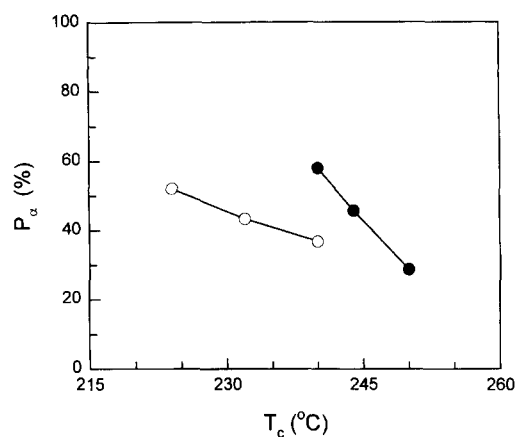


Figure 7 Percentage content of the α -form (P_α) in the crystalline phase versus crystallization temperature (T_c) for pure sPS and the sPS/PPO (80/20) blend. The filled and open circles represent the pure sPS and the sPS/PPO (80/20) blend, respectively

α -form (P_α) was quantitatively evaluated and plotted against T_c in Figure 7. In both pure sPS and the sPS/PPO (80/20) blend, the content of the α -form decreases with increasing T_c . It is worth noting that under the same crystallization temperature, e.g. $T_c = 240^{\circ}\text{C}$, the amount of α -form in the sPS/PPO blend is lower than that in pure sPS. This result indicates that the PPO favours the formation of the β -form, which is consistent with the previous results^{26,27}.

CONCLUSIONS

The sPS/PPO blends show a single T_g over the entire composition range, indicating the miscibility of the blends. When the melting behaviour of both pure sPS and the sPS/PPO blend was examined in detail, both sPS and the sPS/PPO blend showed three melting endotherms under our crystallization conditions. The melting endotherms I and II may be due to the melting of β - and α -forms of the sPS crystal, respectively, while the melting endotherm III comes from the melting of recrystallized sPS formed during the d.s.c. scan. It is also noted that pure sPS recrystallizes more easily than sPS/PPO blends, indicating that the PPO disturbs the recrystallization of sPS.

REFERENCES

- Rim, P. B. and Runt, J. P., *Macromolecules*, 1984, **17**, 1520.
- Chen, H.-L., Hwang, J. C. and Chen, C.-C., *Polymer*, 1996, **37**, 5461.
- Samuel, R. J., *J. Polym. Sci., Polym. Phys. Ed.*, 1975, **13**, 1417.
- Prest, W. M. Jr. and Luca, D. J., *J. Appl. Phys.*, 1975, **46**, 4136.
- Edwards, B. C., *J. Polym. Sci., Polym. Phys. Ed.*, 1975, **13**, 1387.
- Bassett, D. C., Olley, R. H. and Al Raheil, I. A. M., *Polymer*, 1988, **29**, 1745.
- Zachmann, H. G. and Stuart, H. A., *Makromol. Chem.*, 1960, **49**, 131.
- Hybart, F. J. and Platt, J. D., *J. Appl. Polym. Sci.*, 1967, **11**, 1449.
- Todoki, M. and Kawaguchi, T., *J. Polym. Sci., Polym. Phys. Ed.*, 1977, **15**, 1067.
- Ishihara, N., Seimiya, T., Kuramoto, M. and Uoi, M., *Macromolecules*, 1986, **19**, 2464.
- Guerra, G., Vitagliano, V. M., De Rosa, C., Petraccone, V. and Corradini, P., *Macromolecules*, 1990, **23**, 1539.
- Vittoria, V., de Candia, F., Iannelli, P. and Immirzi, A., *Makromol. Chem., Rapid Commun.*, 1988, **9**, 765.

13. Wang, Y. K., Savage, J. D., Yang, D. and Hsu, S. L., *Macromolecules*, 1992, **25**, 3659.
14. Greis, O., Xu, Y., Asano, T. and Petermann, J., *Polymer*, 1989, **30**, 590.
15. Sun, Z. and Millar, R. L., *Polymer*, 1993, **34**, 1963.
16. De Rosa, C., Guerra, G., Petraccone, V. and Corradini, P., *Polym. J.*, 1991, **23**, 1435.
17. De Rosa, C., Rapacciuolo, M., Guerra, G., Petraccone, V. and Corradini, P., *Polymer*, 1992, **33**, 1423.
18. Chatani, Y., Shimane, Y., Inoue, Y., Inagaki, T., Ishioka, T., Ijitsu, T. and Yukinari, T., *Polymer*, 1992, **33**, 488.
19. Chatani, Y., Shimane, Y., Inagaki, T., Ijitsu, T., Yukinari, T. and Shikuma, H., *Polymer*, 1993, **34**, 1620.
20. Roels, T., Deberdt, F. and Berghmans, H., *Macromolecules*, 1994, **27**, 6216.
21. Kellar, E. J. C., Galiotis, C. and Andrews, E. H., *Macromolecules*, 1996, **29**, 3515.
22. de Candia, F., Russo, R. and Vittoria, V., *J. Polym. Sci.: Part C: Polym. Lett.*, 1990, **28**, 47.
23. Cimmino, S., Di Pace, E., Martuscelli, E. and Silvestre, C., *Polym. Commun.*, 1991, **32**, 251.
24. Cimmino, S., Di Pace, E., Martuscelli, E., Silvestre, C., Rice, D. M. and Karasz, F. E., *Polymer*, 1993, **34**, 214.
25. Cimmino, S., Di Pace, E., Martuscelli, E. and Silvestre, C., *Polymer*, 1993, **34**, 2799.
26. Guerra, G., De Rosa, C., Vitagliano, V. M., Petraccone, V., Corradini, P. and Karasz, F. E., *Polym. Commun.*, 1991, **32**, 30.
27. Guerra, G., De Rosa, C., Vitagliano, V. M., Petraccone, V. and Corradini, P., *J. Polym. Sci.: Part B: Polym. Phys.*, 1991, **29**, 265.
28. Gordon, M. and Taylor, J. S., *J. Appl. Chem.*, 1952, **2**, 493.
29. Belorgey, G. and Prud'homme, R. E., *J. Polym. Sci., Polym. Phys. Ed.*, 1982, **20**, 191.
30. Belorgey, G., Aubin, M. and Prud'homme, R. E., *Polymer*, 1982, **23**, 1051.
31. Iriarte, M., Iribarren, J. I., Etxeberria, A. and Iruin, J. J., *Polymer*, 1989, **30**, 1160.